

A Large Neutrino Detector Facility at the Spallation Neutron Source at Oak Ridge National Laboratory

Yu. V. Efremenko (on behalf of ORLaND collaboration)

Physics Division, Oak Ridge National Laboratory,

MS-6372, Oak Ridge, TN 37831-6372, USA

E-mail: efremenk@utkux1.utk.edu

The ORLaND (Oak Ridge Large Neutrino Detector) collaboration proposes to construct a large neutrino detector in an underground experimental hall adjacent to the first target station of the Spallation Neutron Source (SNS) at the Oak Ridge National Laboratory. The main mission of a large (2000 ton) Scintillation-Cherenkov detector is to measure $\bar{\nu}_\mu \rightarrow \bar{\nu}_e$ neutrino oscillation parameters more accurately than they can be determined in other experiments, or significantly extending the covered parameter space below ($\sin^2 2\theta \leq 10^{-4}$). In addition to the neutrino oscillation measurements, ORLaND would be capable of making precise measurements of $\sin^2 \theta_W$, search for the magnetic moment of the muon neutrino, and investigate the anomaly in the KARMEN time spectrum, which has been attributed to a new neutral particle. With the same facility an extensive program of measurements of neutrino nucleus cross sections is also planned to support nuclear astrophysics.

1 The Spallation Neutron Source SNS and ORLaND

The Spallation Neutron Source (SNS) under construction at the Oak Ridge National Laboratory will produce the most intense pulsed-proton beam in the world. It consists of a 493-m long linac, an accumulator ring with a radius of just over 35 meters, and a target station. A second accumulator ring and target station is planned to be built in the future. **The SNS will** be used primarily for material science research. **However,** it also will be the world's most powerful neutrino factory. The high intensity and the pulsed nature of the accumulator ring, provides an ideal laboratory for neutrino physics research at medium energies. The short-pulsed beam ($\leq 0.55 \mu\text{sec}$, 60Hz) provides a virtually cosmic-ray-free measurement of various neutrino interactions. It also permits the separation of neutrinos from pion decay and muon decay. A plan view of the completed SNS facility is shown in Fig 1.

The existence of a second accumulator ring and target station would make SNS a unique neutrino facility with two simultaneously operating sources with known time structures and different flight paths. The final planned beam current (4 mA) and proton energy (1 GeV) will produce neutrino fluxes 10 times as intense as those at LANCE¹, but with a pulse time structure similar to that used successfully by KARMEN at the ISIS neutron source².

Table 1 shows the design parameters of the SNS.

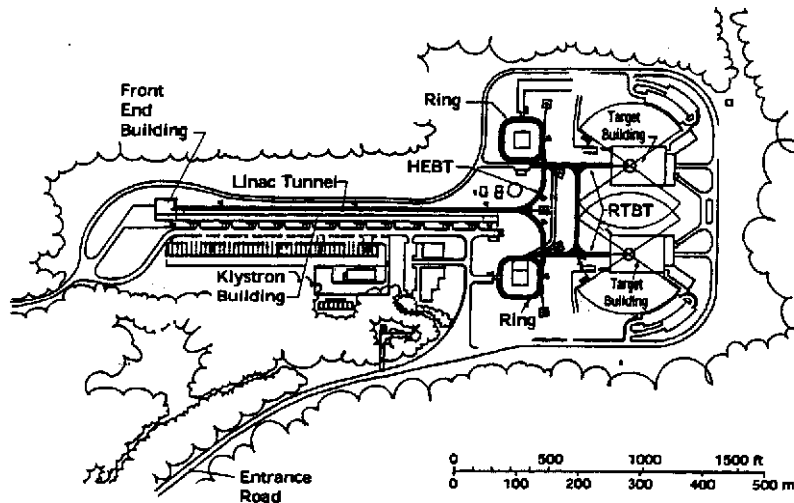


Figure 1: **Plan** view of the completed SNS facility.

The **ORLaND** detector will be placed in a bunker located immediately adjacent to the **SNS** first target building. It will be totally underground, with the top of the concrete cap level with the finished grade of the site. The distance between the center of the **neutrino** detector and the center of the first **SSS** target is approximately 139 feet (**42.3** meters),.

2 **Neutrino** Oscillation Search

2.1 *Search for $\bar{\nu}_\mu \rightarrow \bar{\nu}_e$ oscillations*

The **ORLaND** neutrino oscillation search, similar to LSND and KARMEN is based on a unique feature of **neutrino** beams from spallation sources. The enormous suppression of $\bar{\nu}_e$ production allows the attribution of $\bar{\nu}_e$ events to $\bar{\nu}_\mu \rightarrow \bar{\nu}_e$ oscillation.

This feature has the following explanation. In the **SNS** pions are copiously produced from the interaction of 1.0 **GeV** protons with the mercury target. The production rate is approximately 0.068 π^+ and 0.049 π^- per proton.

Absorption of π^+ and its decay μ^+ are negligible. However most π^- are quickly stopped and captured in the target materials. Detailed simulations

	baseline	after upgrade
beam power on the target	1 MW	4 MW
beam energy on the target	1 GeV	
average beam current	1 mA	4 mA
repetition rate	60 Hz	10 Hz, 60 Hz
ion type, source-linac	H^-	
particles stored in ring (ppp)	1×10^{14}	2×10^{14}
extracted pulse length	550 nsec	
peak current on target	30 A	120 A
number of target stations	1	2
target material	mercury	
beam spot on target	7×21 cm	
neutron moderators	4	8
neutron beam ports	18	36

Table 1: SNS Design Parameters

show that about 99.6% of the negative pions produced in the Hg target, are captured before they have a chance to decay. Moreover, a significant number of μ^- (94%) are captured by heavy elements in the target and in the surrounding lead reflector. This results in a large asymmetry between $\bar{\nu}_e$ and $\bar{\nu}_\mu$ production. In Fig. 2, and Fig. 3 the calculated time and energy spectra for four types of neutrino are shown. Several conclusions can be drawn from these distributions:

1. There is a large imbalance between the two antineutrino flavors in favor of $\bar{\nu}_\mu$.
2. Most of the $\bar{\nu}_\mu$ are produced from decay at rest (DAR) due to the large stopping power in heavy and dense target materials. Production of high-energy $\bar{\nu}_\mu$ (above 52.83 MeV kinetic energy) is due to the decays in flight (DIF). This production is suppressed by the design of the spallation target station, the large size of the mercury target, and the lead reflector.
3. There is a strong time dependence of the $\bar{\nu}_e$ to $\bar{\nu}_\mu$ ratio. This is because of the fast capture rate of μ^- in the high Z materials (mercury in the target and lead in the neutron reflector). This time dependence allows us to experimentally measure background from $\bar{\nu}_e$, which is the largest beam-related irreducible background.

Based on detailed simulations for the SNS target station, we concluded that the ratio of $\bar{\nu}_e$ to $\bar{\nu}_\mu$ in ORLAND will be $2.4 \cdot 10^{-4}$, three times smaller than the ratio calculated for the LSND experimental setup.

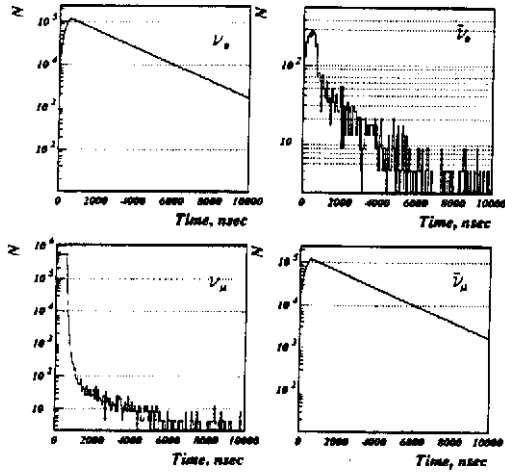


Figure 2: Time distributions for four neutrino types produced at SNS.

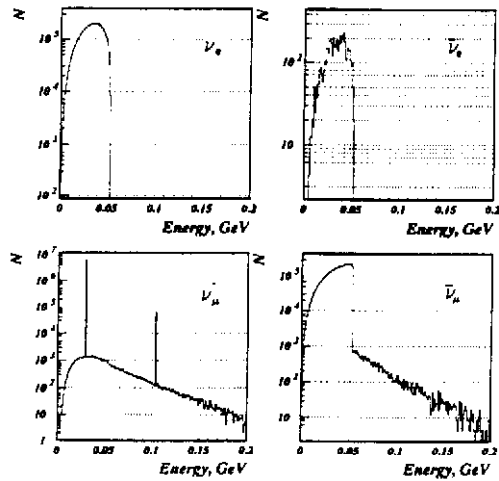


Figure 3: Energy distributions for four neutrino types produced at SNS. The monoenergetic line for the muon neutrino near 100 MeV does not include broadening due to nuclear effects.

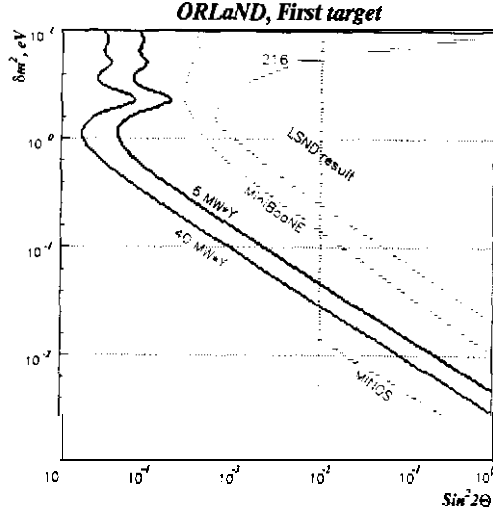


Figure 4: Limits for mixing parameters for neutrino oscillations reachable at ORLaND compared with that of Mini-BooNE, MINOS and I-216 proposals

In Fig. 4 the possible limits for neutrino oscillation parameters for ORLaND are compared with that of LSND, Mini-BooNE, MINOS, and CERN I-216 proposals. For ORLaND two limits with the first target station are shown. One results from the first three years of operation with integrated intensity of 6 MW*Y. The second one corresponds to the limits achievable over the life time of facility 40 MW*Y. The ORLaND will not only cover the entire region where LSND indicates an oscillation effect but will probe a significantly larger area of possible mixing parameters. Compared with Mini-BooNE, ORLaND will have almost an order of magnitude better sensitivity in both mixing angle and δm^2 and with much less background.

The very intense SNS-based neutrino source together with the massive size of the ORLaND detector provides an unprecedented opportunity for a high-statistics neutrino oscillation search. In one week the ORLaND detector will be able to accumulate the same statistics as LSND did in three years. If LSND results are confirmed by early experiments (KARMEN, Mini-BooNE), ORLaND would be uniquely positioned to measure precisely the neutrino mixing parameters. An example of such a measurement is shown in Fig. 5. The mixing parameters $\sin^2 2\theta \approx 1.5 \cdot 10^{-2}$ and $\delta m^2 \approx 0.7$ eV were assumed in this figure. For one year of data taking with spallation power of 1 MW per

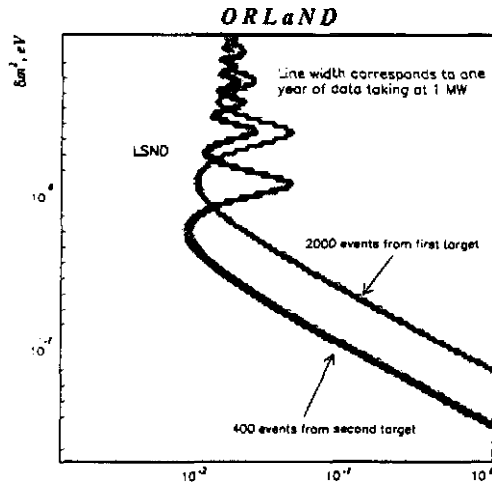


Figure 5: The precision of the **measurement** of the mixing parameters in the LSND region. Narrow bands correspond to regions of allowed parameters, using the number of events from the first and second target stations for one year of data collection with a **spallation** source power of 1 MW per target.

target **ORLaND** will detect 2,000 events from the first and 400 events from the second **spallation** target. Corresponding regions of allowed parameters are shown by the two narrow bands. The intersection of these bands corresponds to the accuracy of measurement of the mixing parameters.

2.2 Search for $\nu_\mu \rightarrow \nu_e$ transitions with monoenergetic neutrinos

The time structure and monoenergetic character of the spectrum of ν_μ due to the decay $\pi^+ \rightarrow \mu^+ + \nu_\mu$, shown in Fig. 2 and Fig. 3, can be used in **ORLaND** to search for $\nu_\mu \rightarrow \nu_e$ oscillations. These neutrinos **will** oscillate to ν_e with an observable probability for **some** values of $\sin^2 2\theta$ and δm^2 in the range reported by the LSND collaboration. The reaction $^{12}\text{C}(\nu_e, e^-) ^{12}\text{N}_{g.s.}$ results in a **Cerenkov** ring, followed by the decay $^{12}\text{N}_{g.s.} \rightarrow ^{12}\text{C} + e^+ + \nu_e$. There will, of course, be a background of ν_e from the broad spectrum due to the decay of μ^+ ; however, it will be suppressed by making use of the time structure of the neutrinos shown in Fig. 2. The events that occur due to $\nu_\mu \rightarrow \nu_e$ oscillations would **cause** a significant distortion of the background spectrum as shown in Fig. 6.

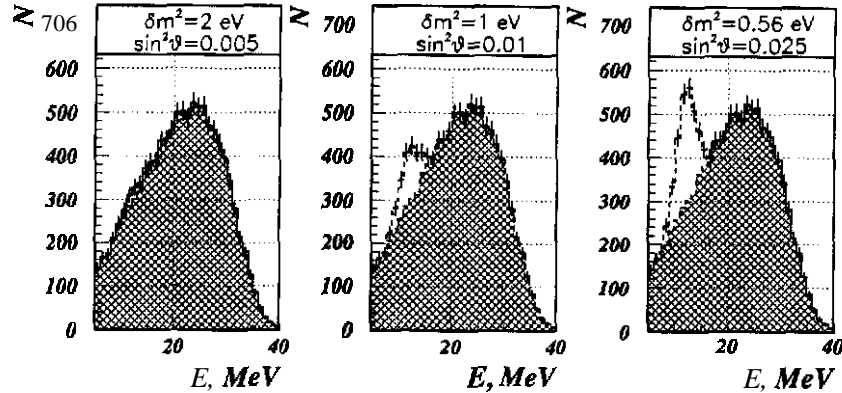


Figure 6: The energy spectrum of electrons from the reaction $^{12}\text{C}(\nu_e, e^-)^{12}\text{N}_{gs}$. The cross-hatched region contains events due to ν_e from the decay of μ^+ . The distributions at the lower energy edge are those predicted for ν_μ to ν_e oscillations for 3 years of data acquisition with ORLaND with a proton beam of 2 mA.

Detection of neutrino oscillations for both neutrinos and antineutrinos, will give the possibility to test CP invariance in the neutrino sector.

3 Other Neutrino Physics at ORLaND

3.1 Measurement Of Neutrino-Nucleus Cross Sections

The similarity of the neutrino spectra from π^+ and μ^+ decay at rest at the neutron spallation source, and those produced during supernovae core collapse is striking. This coupled with the intensity and pulse structure at the SNS makes the proposed ORLaND facility ideal for making measurements that directly support theoretical nuclear astrophysics.

Supernovae involve such a large number of neutrino-nucleus reactions, some involving radioactive nuclei, that laboratory measurements of all of them are impossible. Accordingly, random phase approximation models are used³, which themselves have parameters. It is important to test and tune these models in a few important cases which can be measured in the small segmented detector planned for the ORLaND facility. In this detector, materials foreign to the scintillator can be introduced in a variety of ways.

3.2 Precision $\sin^2\theta_w$ Measurement Using $\nu - e$ Elastic Scattering

The high intensity of the SNS neutrino beam in combination with its unique time structure will let ORLaND measure $\sin^2\theta_w$ with an accuracy approaching 1%.

Measurements of the masses of the intermediate vector bosons made in the past few years provide the most accurate determination of the parameter $\sin^2\theta_w$. However two independent measurements performed at LEP and SLAC differ by more than 1.80. This contradicts the prediction of the SM that $\sin^2\theta_w$ is the sole parameter in this theory. It is important that $\sin^2\theta_w$ be tested with neutrinos as a probe with higher possible accuracy. Deep inelastic scattering on nucleons has proved to be the most accurate method so far but it has the problem common to hadronic processes that calculation of the result involves theoretical uncertainties at the level of a few percent. Neutrino-electron scattering experiments have been limited in the past by lack of statistics, subtraction of background, and difficulties in the neutrino flux calculations. The most precise neutrino-electron measurements have been of the ratio of neutrino to antineutrino scattering. A substantial contribution to the systematic error in these experiments arises from the uncertainty in the characteristics of the two neutrino beams. We propose to measure the ratio,

$$R = \frac{\sigma(\nu_\mu e)}{\sigma(\nu_e e) + \sigma(\bar{\nu}_\mu e)} = \frac{3}{4} \frac{1 - 4s^2 + 16/3s^4}{1 + 2s^2 + 8s^4} \quad (1)$$

where $s^2 = \sin^2\theta_w$. For $\sin^2\theta_w = 0.23$, $R = 0.13$

ORLaND, therefore, proposes to make a precision measurement of the ratio of neutrino electron scattering with neutrinos from pion decay and muon decay simultaneously.

We have estimated errors on the basis of a two-kiloton detector located 42 meters from the beam-stop. For three years of data taking at SNS intensity of 2 MW there will be about 50 000 ($\nu_e e$) and 9 000 ($\nu_\mu e$) and ($\bar{\nu}_\mu e$) interactions in the detector. These statistics will let us measure $\sin^2\theta_w$ with an accuracy close to 1%. Of course intensive studies will be required to evaluate the magnitude of systematic errors.

3.3 KARMEN's Anomalous Bump on the Time Decay Curve

In 1995 the KARMEN collaboration reported an anomaly in the time distribution" of neutrinos from the pulsed neutron spallation source ISIS. The anomaly is a peak with a width of 1 μs at 3.6 μs after the beam pulse, on top of the $\tau = 2.2\mu\text{s}$ time spectrum of neutrinos from muon decays at rest. The anomaly

has been observed only in *single* pronged events below 35 MeV. Above this energy the time spectrum is flat. The time distribution of the sequential charged current reaction $^{12}\text{C}(\nu_e, e^-)^{12}\text{N}_{gs}$ showed the expected 2.2 μs decay time, thus indicating that the anomaly is not caused by a variation in muon production or decay. After investigating and excluding several possible sources for this effect, like albedo neutrons from a hill behind the experiment, electronics, and others, KARMEN proposed as a working hypothesis a heavy weakly interacting neutral particle X produced in pion decay: $\pi^+ \rightarrow \mu^+ + X$ with velocity $\frac{1}{80}c$ (17.6m/3.6 μs), having a very small kinetic energy, which leaves 33.9 MeV for the rest mass of the particle. This particle would not be observed directly in the detector, but would decay for example into $\gamma + \nu$ or $e^+ + e^- + \nu$. The detectable decay products would then give a broad energy spectrum between 0 and 33.9 MeV. Since this is the same energy range as for CC and NC neutrino reactions with ^{12}C , the small number of events can not be separated from the normal neutrino background. The excess events have been observed over a time period of 7 years. After a major upgrade of the KARMEN Veto system in 1996, which also involved significant changes in the passive shielding of the detector, the number of events is still increasing with the same rate⁵. However with the low statistics of this effect it will take another two years to verify with 5 σ that it is not a statistical fluctuation

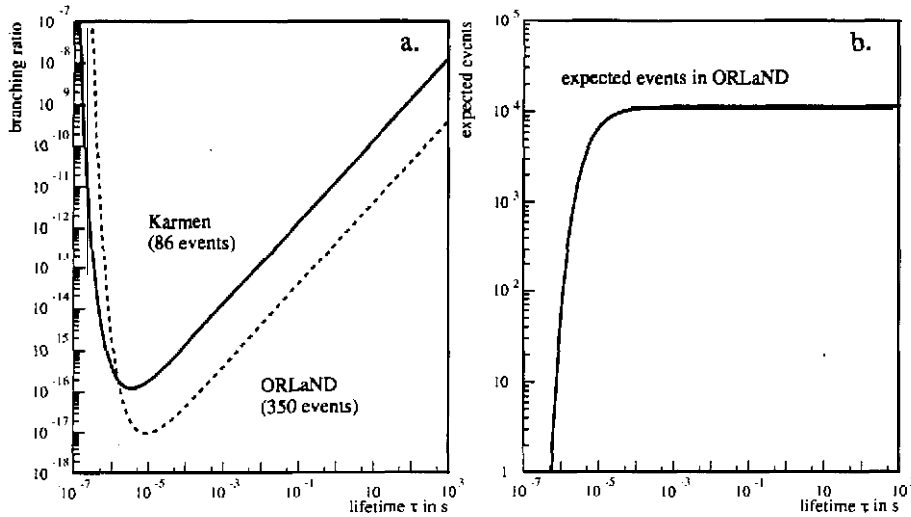


Figure 7: (a) Branching ratio of the Pion decay versus lifetime of the X particle. The dashed curve shows the sensitivity of ORLaND for 350 events. (b) Expected events for X particle in ORLaND, based on the KARMEN result for 4 MW Year of data taking.

ORLaND would be able to look for this effect with much higher statistics. Since ORLaND is farther away from the target, the X particle would be observed in a time window between 8.1 and 9.4 μs , outside the normal neutrino background. Fig. 7 shows the lower limit of the parameter range and expected events rate in ORLaND for lifetimes of X from 10^{-7} to 10^3 sec.

3.4 Search for Effects of the Magnetic Moment of the muon neutrino

The existence of neutrino **mass** leads to the possibility for Dirac type neutrinos to have a magnetic dipole moment or non-diagonal magnetic transition moments for **Majorana** neutrinos. In that case neutrino interactions include an electromagnetic part in addition to the standard weak interaction. The electromagnetic part has a characteristic energy behavior with an increase of the differential cross section, while the recoil energy of the scattering target decreases. The simplest way to measure the neutrino magnetic moment would be to measure the excess of neutrino differential cross section in the low energy of the recoil particle region. From this point of view the ORLaND neutrino facility is not competitive to measure the electron neutrino magnetic moment as compared to reactor neutrino experiments. However, for muon neutrinos, there might be a unique opportunity to improve the existing restriction on the magnetic moment, $\mu < 7.4 \cdot 10^{-10} \mu_B$, by about an order of magnitude.

4 Acknowledgements

This work was supported in part by U.S. Department of Energy under contract DE-AC05-96OR22464 with Lockheed Martin Energy Research Corporation.

1. C. Athanassopoulos et al, PRL **81**; **1774** (1998)
2. B. Armbruster et al, PLB 348, 19 (1995) (the KARMEN collaboration)
3. E. Kolb, K.-H. Langanke, S. Krewald, and f.-K. Thielemann, NBA **A540**, 599 (1992)
4. Armbruster et al., PLB 348, 19 (1995)
5. **Karmen** collaboration, private communication 1998.